ELSEVIER

Finite Elements in Analysis and Design 37 (2001) 843–860

FINITE ELEMENTS IN ANALYSIS AND DESIGN

www.elsevier.com/locate/finel

Experiences in reverse-engineering of a finite element automobile crash model

Z.Q. Cheng[a], J.G. Thacker[a], W.D. Pilkey[a,*], W.T. Hollowell[b], S.W. Reagan[a], E.M. Sieveka[a]

[a] *Automobile Safety Laboratory, University of Virginia, Charlottesville, VA 22904, USA*
[b] *National Highway Traffic Safety Administration, 400 7th St. SW, Washington, DC 20590, USA*

Abstract

The experiences encountered during the development, modification, and refinement of a finite element model of a four-door sedan are described. A single model is developed that can be successfully used in computational simulations of full frontal, offset frontal, side, and oblique car-to-car impacts. The simulation results are validated with test data of actual vehicles. The validation and computational simulations using the model show it to be computationally stable, reliable, repeatable, and useful as a crash partner for other vehicles.

1. Introduction

A major concern of both industry and government in the development of vehicles that would consume less fossil fuel is the possible compromising of occupant safety resulting from the reduced weight and structure of the vehicle. To help researchers assess safety issues of these new cars, several detailed, dynamic finite element (FE) models of vehicles representing today's highway fleet were developed. These models can be used as "crash partners" for other models developed by automobile manufacturers. They also provide detailed models for use in studying the crash behavior of automobile structures.

A finite element model of a four-door 1997 Honda Accord DX Sedan, as shown in Fig. 1, was created at the Automobile Safety Laboratory of the University of Virginia [5]. The model was developed from data obtained from the disassembly and digitization of an actual automobile using a reverse engineering technique. This approach was necessary because

* Corresponding author.
E-mail address: wdp@virginia.edu (W.D. Pilkey)

0168-874X/01/$ - see front matter
PII: S0168-874X(01)00071-3

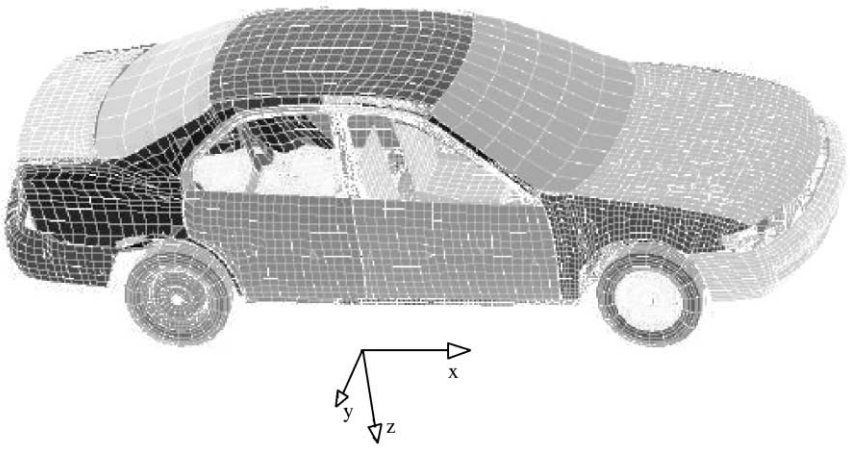

Fig. 1. The original finite element model of the 1997 Honda Accord.

the models developed by the manufacturers are proprietary, and are not available to either the public or to the government.

This paper addresses the efforts to refine the structure of the model, to improve the computational performance of the model, and to validate crash responses of the model with crash test data of actual vehicles. This resulted in a single model that successfully simulates full frontal, offset frontal, side, and oblique car to car impacts. The experience and results of the model modification, refinement, and validation are briefly described.

2. Model structure modification and refinement

In the model, there are hundreds of individual parts that are connected to make up the automobile structure. Although extensive efforts were made to ensure accuracy during this first modeling process, some inevitable deficiencies were still present in the vehicle after all of the parts were reassembled. These included:

- *Missing parts*: Not every part in the actual car, such as fasteners, mouldings, decorating parts, etc., needs to be present in the finite element crash model. However, parts located in major load transmission paths must be accounted for.
- *Connection problems*: In the actual car, parts are connected through thousands of welds, fasteners, adhesive, springs, and dampers. In the model, parts are connected using rigid links, spot welds, springs, and dampers.
- *Initial penetrations*: An initial penetration is an overlap between two parts at the start of the simulation. Small initial penetrations are normal due to the fact that the mesh is only an approximation to the actual structure. In most cases, LS-DYNA [4] can automatically adjust nodes during its initialization process so that such penetrations are eliminated. Sometimes, however, large penetrations remain. This can occur, for instance, when one part cuts through another part at a large angle. No matter which direction LS-DYNA tries to move the nodes in

question, a penetration will remain. Another situation can involve three shell layers that are nearly parallel and very close together. Resolving the penetration between the interior shell and one of the exterior shells can create new contacts with the other exterior shell. Cases such as these must be corrected manually. Large penetrations result in high initial stresses in the penetrated parts.

- *Material property issues*: There are over 200 parts in the model. While the material properties of the steel alloys are well known, the properties of some materials, such as honeycomb, foam, and plastics are not readily available. In particular, some of these materials undergo large changes in volume when loaded, and exhibit highly non-linear behavior. These factors can lead to some persistent computational problems.

The modification and refinement of the model is essentially a trial-and-error process which can be very inefficient and time-consuming. In an effort to rectify the above issues, the following procedures are taken.

2.1. Static review

With the aid of the pre-processing software, HyperMesh [3], the model is reviewed statically before the simulation is initiated. The issues dealt with during this review included:

- *Element quality*: Major issues related to one-dimensional elements (spot welds and rigid links in particular for this model) include free-ends, rigid loops, dependency, connectivity, and duplicates. The issues associated with two- and three-dimensional elements involve element warpage, aspect ratio, skew, and Jacobian.
- *Part association*: This association indicates the connections (spot weld and rigid link) and relative position (penetrated, attached, or separated). While penetrations can be manually detected using three-dimensional part viewing, a more efficient way to find penetrations is by examining the initial stress distribution of the model prior to impact.
- *Concentrated mass distribution*: In the model, concentrated masses (point masses) were used to represent parts like fluid reservoirs that are not substantial to impact load, test instrumentation that is not in the primary crash zone, and anthromophic test devices that are not modeled in this study. Since high accelerations are generated during impact, inertial effects of point masses are very significant.
- *Summary information*: Information such as the mass and the CG (center of gravity) of each part and the entire model can be found from the static review and is compared to the actual test vehicle.

2.2. Initial stress check

The initialization of the model in a computational simulation provides information including the initial stress distribution. Using the initial stress distribution, one can easily identify the parts with large penetrations.

2.3. Gross motion

Gross motion reveals the overall dynamic response of the model and is akin to rigid body motion. The gross motion of the physical vehicle is found from the VHS video tape recorded by the National Highway Traffic Safety Administration (NHTSA) during each test. The comparison of the gross motion of the test vehicle and computer model was used to initially define major problems. The gross motion of the vehicle also provides a simple way to detect parts or part-group that are improperly connected to the main structure. While this motion reveals the global dynamic behavior of the vehicle, it is too coarse to be used for acceleration validation.

2.4. Acceleration responses

After all obvious problems in the model had been resolved, and the gross motion and deformation of the model were similar to those of the test vehicles; the matching of acceleration responses from the model with test signals became the central focus. Acceleration responses are available as output at all model nodes, but comparisons can only be made at locations instrumented in the test. The standard locations for a full-frontal test are on the top and bottom of the engine, at the CG of the vehicle, and on the left and right sides of the rear cross member.

2.5. Post-test observations

Post-test observations (usually included in a NHTSA test report) provide information about the permanent deformations at several locations of the tested vehicle. The permanent deformations can also be reviewed from the test video. This information is useful for model modification and refinement, especially for those parts with large permanent deformations. During the validation of the model for side impact, the impact dynamic behavior of a movable deformable barrier (MDB) was of key importance. The post-crash deformations of the MDB model in computer simulations with the post-test observations of an actual side impact test [1] were utilized to improve the MDB model structure and properly set the honeycomb material property from which the impacting part of the MDB was constructed.

3. Computational issues of model simulations

Several major computational issues associated with LS-DYNA and the model need to be addressed.

3.1. Negative volume of solid elements

Premature program termination due to the negative volume of solid elements was frequently encountered. Computationally, this is due to the calculation of the element Jacobian at geometric points outside the boundary of highly deformed solid elements. If soft materials, such as honeycomb and foam, were used for a solid element part, rapid compression of the elements

will likely result and negative volumes would be computed. The following parts of the Accord model often caused negative volume problems resulting in premature termination of the simulation:

- *Radiator*: a solid element part made from crushable foam.
- *Seat cushions*: solid element parts made from low density foam.
- *The deformable barriers*: solid element parts made from honeycomb material; used in side impact and offset frontal impact simulations, respectively.

Major factors that are related to the improvement of the negative volume problem included:

- *Element size*: Computational experiments indicate that the smaller the element size of highly deformed parts, the more likely the occurrence of negative volume calculations. Increasing element size has proven to be an effective method in resolving this problem. Element size has an upper limit, however, if realistic modeling is to be accomplished.
- *Material property*: In a broad sense, the stress–strain relationship for the foam (low density foam and crushable foam) and honeycomb materials are defined by load curves. When the relative volume (the ratio of current to initial volume) of a solid element becomes very small, the slope of a load curve could be a major negative volume producing factor.
- *Interior contact setting*: Setting an interior contact for a solid element part is found to increase the stiffness of that part, which aids in reducing the negative volume problem for that part. However, it seems reasonable that this setting would significantly alter the impact behavior of the part.
- *Hourglass*: One aspect that leads to negative volume problems is the deformation of elements in an hourglass mode. Therefore, using the LS-DYNA solid element hourglass control helps to avoid hourglass-mode deformations and thus reduce negative volume problems.

3.2. Shooting nodes

Another frequently occurring computational problem was a termination due to mass increase. That is, the percentage increase of the added mass has reached a prescribed limit. Although LS-DYNA defines this termination as a normal termination, it usually happens before the completion of the prescribed run time, or even at a very earlier stage of a simulation process. It is actually a computational instability. The animation of dynamic responses of the model shows that the deformations of certain elements in one or more parts continue to increase to unrealistically large displacements. It appears as though certain nodes are ejecting or "shooting" out of the model as deformations develop. In LS-DYNA, the time step size roughly corresponds to the transient time of an acoustic wave through an element using the shortest characteristic distance. Shooting nodes result in drastic decrease of the shortest element characteristic distance. Mass scaling is done to meet the Courant time step size criterion [4]. The known factors that lead to, or have effects on, the shooting node problem are as follows.

- *Poor mesh quality*: In many cases, shooting nodes occur in poorly meshed parts. The parts that have large warpage, skew ratios, and high aspect ratios are more likely to have shooting nodes. One explanation for this is that for nonlinear finite element analysis, poor element

characteristics will more likely result in computational instabilities. Usually, after reconstruction and improving mesh quality, shooting nodes disappear, but not always.

- *Redundant elements*: For the Accord model, the meshing of most parts was generated automatically from the digitized line and surface data. Due to errors and bias in the digitized data, redundant elements were sometimes created. If the nodes of a redundant element are not fully connected, that is, one or more nodes are freely ended, these nodes might displace wildly while the region of this part and this redundant element are deforming. Therefore, checking for, and removing, all redundant elements helps to avoid the shooting node problem.
- *Hourglassing*: To keep the computational time acceptable element formulation-2 in LS-DYNA (Belytschko–Tsay element) was used for most shell elements. The standard B-T element is a four-node quadrilateral with a single Gaussian integration point at the center. This under-integration can lead to the occurrence of zero-energy hourglass modes. A hourglass mode is another computational instability [2]. In some cases, the deformation of elements with shooting nodes relates to an hourglass mode. The hourglass mode can be controlled by introducing an artificial viscosity to damp out the oscillations [4]. Using the hourglass control has helped to eliminate shooting node problems. However, for the parts with poor meshing quality, redundant elements, and improper connections, using the hourglass control will only delay the occurrence of shooting nodes.
- *Plastic failure of material*: The primary material definition used in the model was MAT_PIECEWISE_LINEAR_PLASTICITY. Usually, EPPF = 0 (plastic failure is not considered) and TDEL = 0 (element will not be automatically deleted according to minimum time step size) are set in the material card. This material selection was found to be appropriate for parts subject to compressive deformation. Some parts, however, were subject to tensile deformation during the impact and shooting nodes were found more often in this mode. Under compression, parts are pressed together and cannot really "fail" the way they can under tension; so it is appropriate to turn off the normal failure criteria. Under tension, however, it is not realistic to prevent failure since this can allow such a part to experience extreme elongation which leads to shooting nodes. If plastic strain failure or minimum time step size is set for these parts, the elements containing shooting nodes will be automatically deleted. This reduces added mass requirements and the computational process continues.

3.3. Energy balance

The overall model energy balance was used as a measure of FE model quality. Typically, it is thought that the increase of the total energy over the initial energy should be less than 10% and the ratio of the hourglass energy to the total energy be less than 10%. The increase of the total final internal energy over the total initial kinetic energy is affected by the definitions of certain material properties in the model. Fig. 2 illustrates internal and kinetic energies of the front bumper in two cases. In one case, plastic failure is not considered (EPPF = 0 is set in the material card). In another case, the material fails when its plastic strain reaches 200% (EPPF = 2.0), and failed elements will be deleted automatically. The load curve (stress versus strain) for this material usually remains flat in the plastic region. If plastic strain failure is not prescribed, once the stress reaches this plateau, the strain will continue to increase as long as a load is applied. Since the work done in deforming a part is proportional to the product of stress

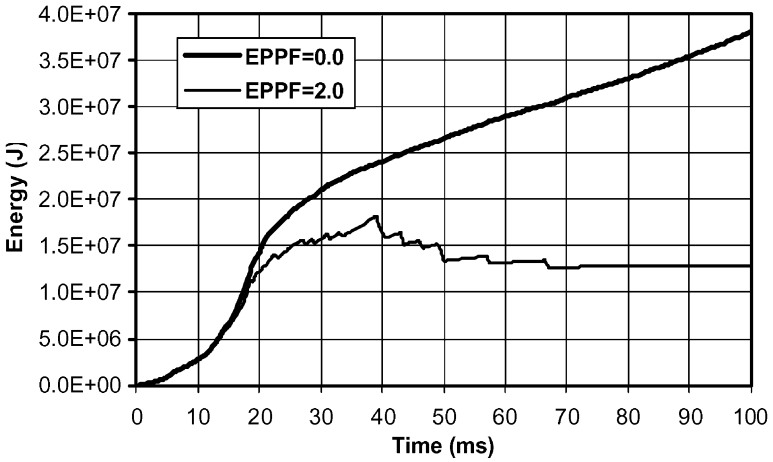

Fig. 2. The internal energies of the frontal bumper for different setting of EPPF.

and strain, this will cause the internal energy to increase for the remaining time of the impact, as illustrated in Fig. 2. However, if plastic strain failure is set for the material, an element will be deleted if its plastic strain exceeds the failure limit; thus preventing the further increase of internal energy. It should be realized, however, that new loading conditions will occur after the deletion of failed elements.

The total hourglass energy is affected by the hourglass coefficient QH that can be set via the CONTROL_HOURGLASS card in LS-DYNA. As the value of QH decreases, the total hourglass energy decreases, as indicated by Fig. 3. However, as stated above, since most shell elements are of the under-integrated type, sufficiently larger values of QH are necessary to prevent hourglass-mode deformations. As a trade-off, a small QH may be used for the entire model while a sufficiently large QH is used for those parts that cause problems. In the model, QH values of 0.040–0.10 were set for the entire model, while the hourglass coefficient $QM =$ 0.1–0.14 was used individually for the solid element parts with foam or honeycom materials as well as some shell element parts that seemed to be subject to large extension deformations.

Hourglass-mode deformations still occurred in certain components even though large hourglass coefficients were used for them. One way to reduce the hourglass energy is to change the element formulation from an under-integrated to a fully integrated type. A fully integrated element formulation results in zero hourglass energy for a part at a higher computational cost. Another way is to improve the element quality of a part, which will not completely eliminate the hourglass energy. It was found that the acceleration responses of the model are not sensitive to the hourglass energy change over a certain range. Fig. 4 illustrates the acceleration responses at the left rear cross member in the full frontal 35 mph impact simulations of two models with different element formulations. In Model A, the element formulations of all parts were under-integrated. In model B, the element formulations were changed into fully integrated for the parts in major load transmission paths. While the total hourglass energy was reduced by 21.5% (from 32.82 kJ to 25.78 kJ for Model A to Model B), the variations of the acceleration responses were not significant.

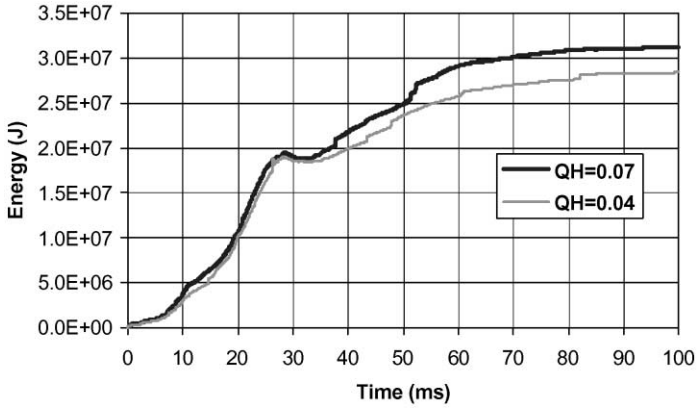

Fig. 3. The variation of the total hourglass energy vs. QH.

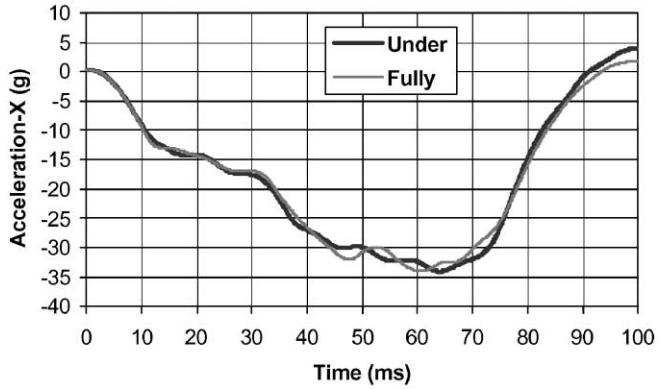

Fig. 4. Comparison between fully and under integrated element formulations (left rear cross member).

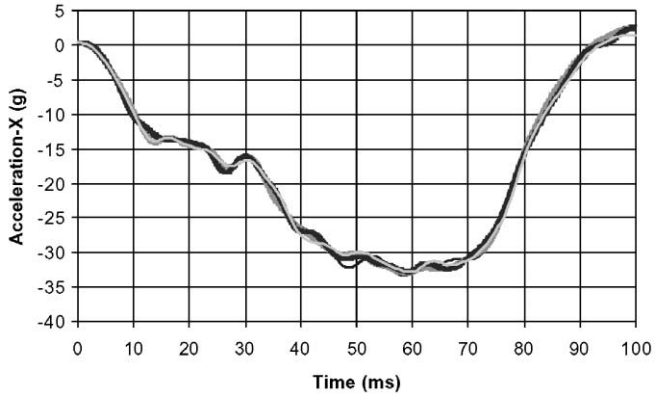

Fig. 5. Acceleration calculation using rigid body acceleration data (left rear cross member in four repeated simulations).

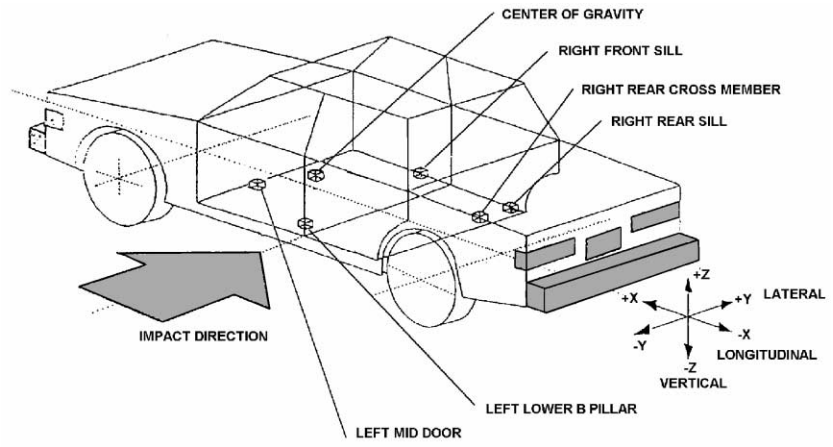

Fig. 6. Locations of accelerometers of side impact test.

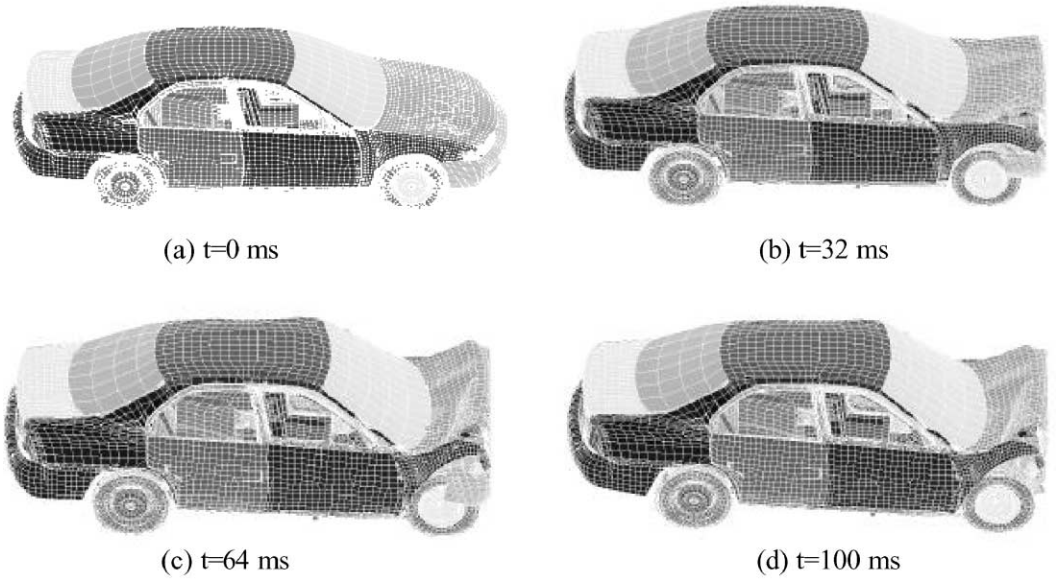

Fig. 7. The gross motion of the model in a full frontal 35 mph impact simulation.

3.4. Calculation of accelerations

To validate the model, the acceleration responses of the model were compared with physical test data at specified locations. Experience showed that different methods of calculation resulted in significant variations of acceleration responses. Originally, the calculation of accelerations of the model was accomplished by averaging the accelerations of a group of nodes from the region of a part where an accelerometer was placed in the physical test. The results were sensitive to the selection of nodes. Also, there were large variations of the results when the

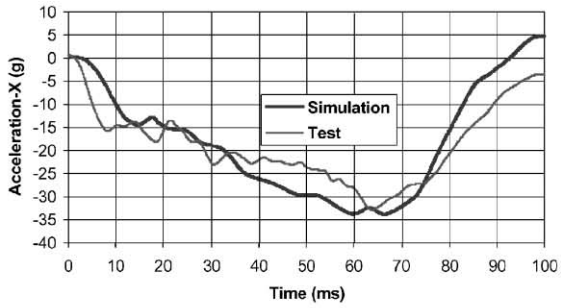

(a) Left rear cross member

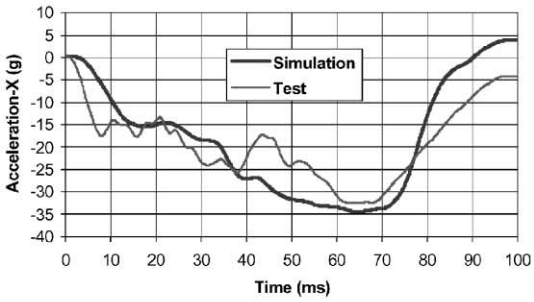

(b) Right rear cross member

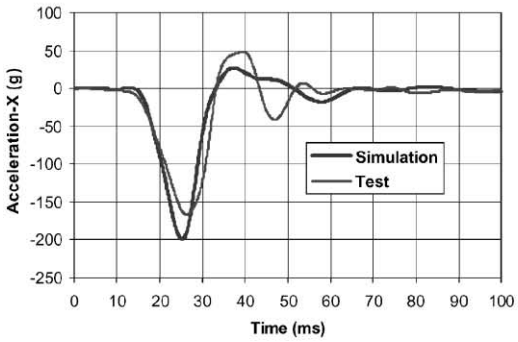

(c) Top of engine

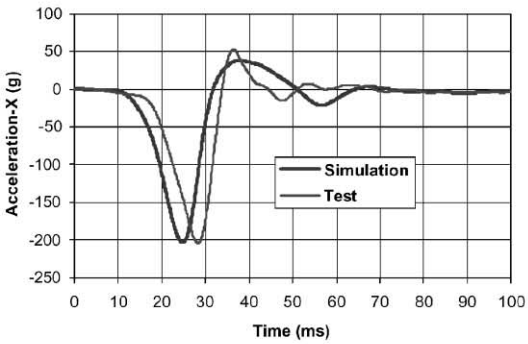

(d) Bottom of engine

Fig. 8. Acceleration validation for the full frontal 35 mph impact.

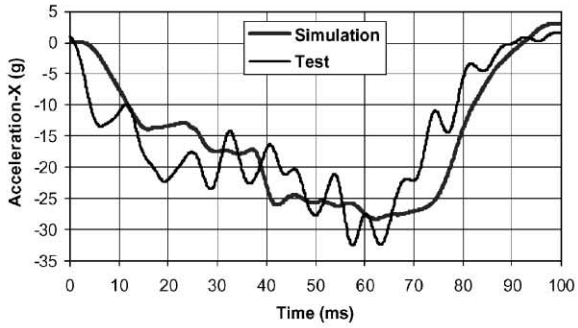

(a) Left rear cross member

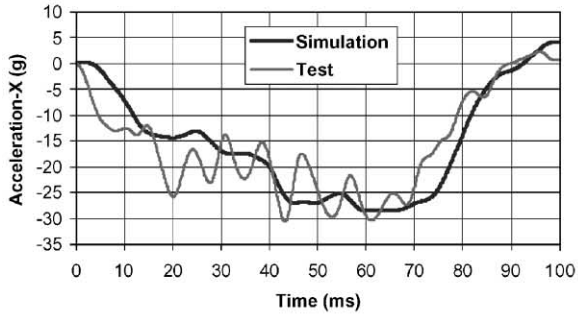

(b) Right rear cross member

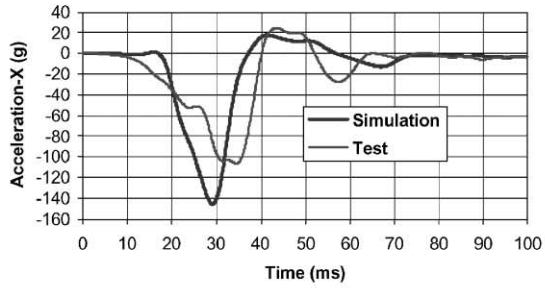

(c) Top of engine

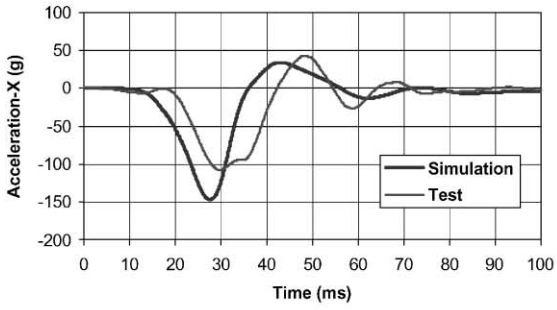

(d) Bottom of engine

Fig. 9. Acceleration validation for the full frontal 30 mph impact.

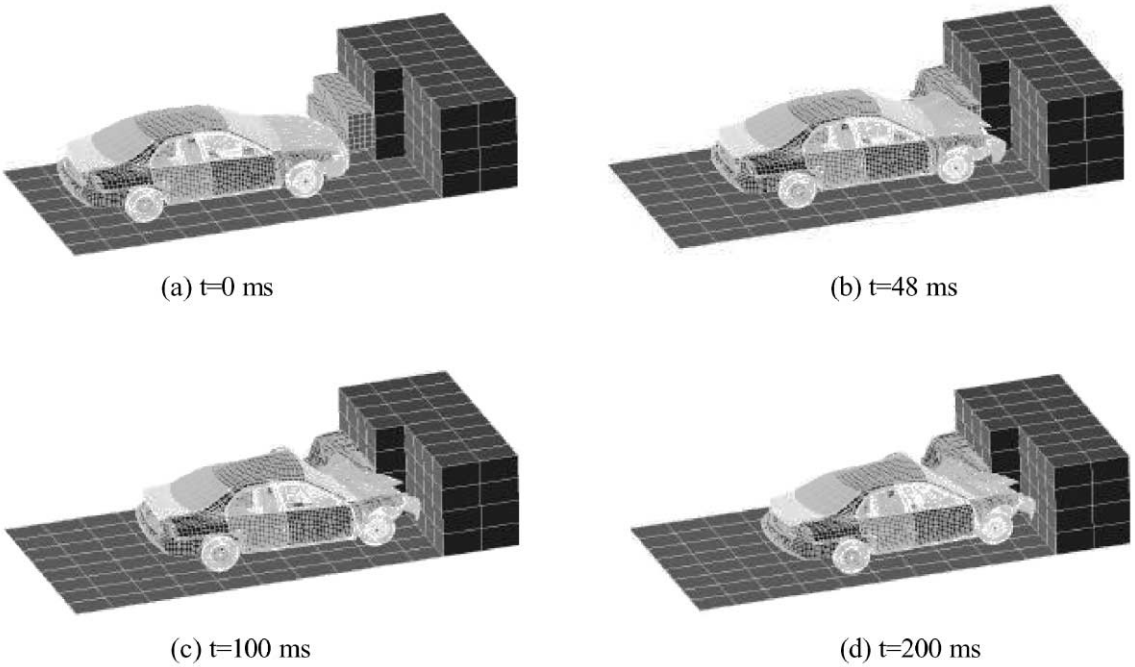

Fig. 10. The gross motion of the model in an offset frontal 40 mph impact simulation.

same model was repeatedly simulated in a multi-processor environment. As an improvement, a model of an accelerometer was created in the model. The modeled accelerometer was represented by a 40 mm rigid cube with a mass of 64 g. This cube was modeled using a solid element with a rigid material. The attachment of this cube to a particular car part was via CONSTRAINED-EXTRA-NODES, where four to eight nodes were selected from different elements of that part around the desired location. The calculation of the acceleration based on the modeled accelerometer was made by selecting two diagonal nodes of the cube and then using the average of the data of these two nodes. While this method of calculation is better than the previous one, there were still significant variations of the results for repeated simulations. A second method was to use the rigid body acceleration data of an accelerometer provided by LS-DYNA. In the MATSUM file, an output file of LS-DYNA, each accelerometer is treated as a part and its rigid body acceleration data is recorded. If these rigid body accelerations were presented as the simulated output signals of the accelerometers in the model, results proved to be stable and repeatable. Fig. 5 illustrates, as an example, the acceleration responses of the left rear cross member in four repeated simulations, where the rigid body acceleration of the accelerometer was presented as its simulated output signal.

4. Crash simulations and validation

The same Accord model is used in all of the following crash simulations. The coordinate system used in the model is shown in Fig. 1. The measurement locations of the vehicle structural

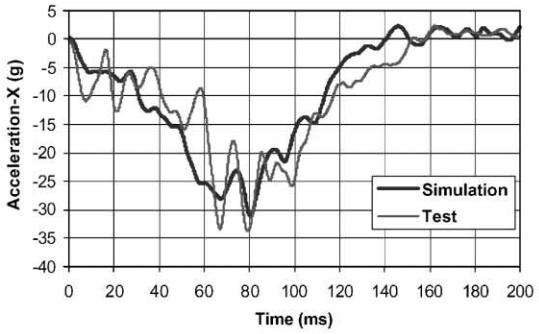

(a) Center of gravity—X

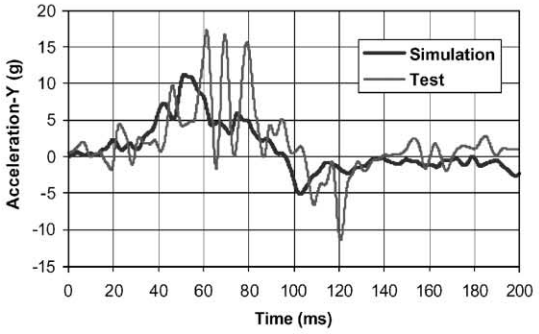

(b) Center of gravity—Y

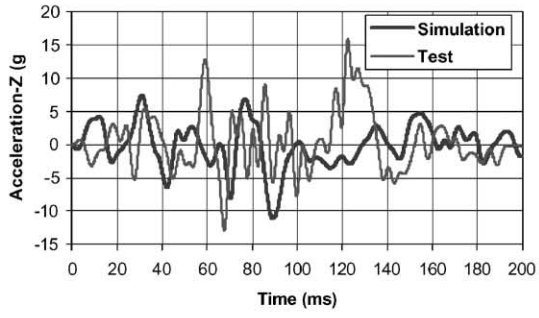

(c) Center of gravity—Z

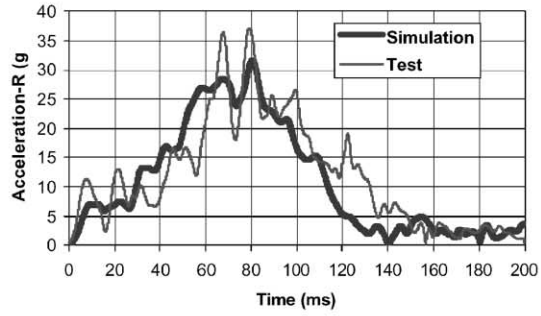

(d) Center of gravity—Resultant

Fig. 11. Acceleration validation for the offset frontal 40 mph impact.

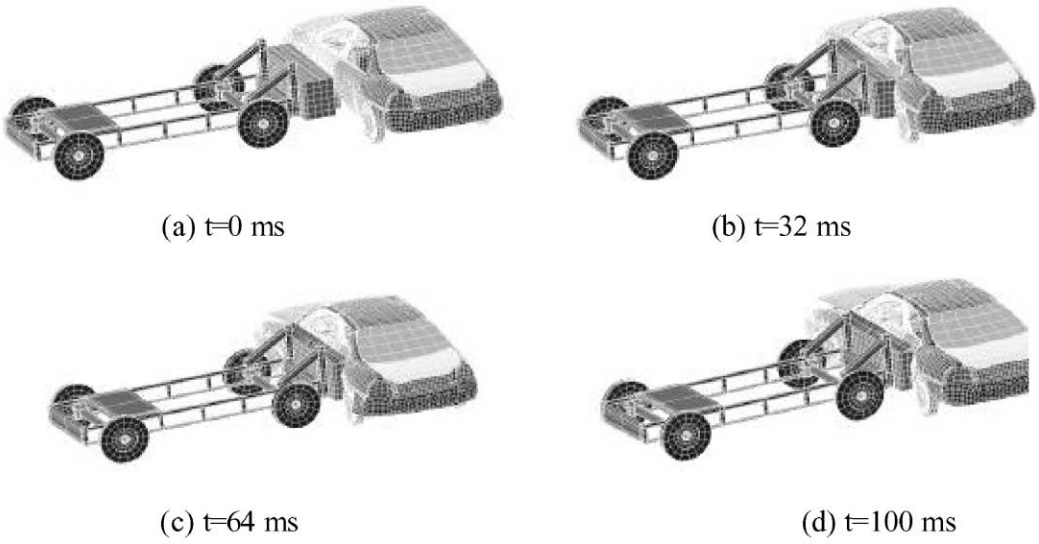

Fig. 12. The gross motion of the model in a MDB 38 mph side impact simulation.

responses in a side impact test is illustrated in Fig. 6 [1]. Both test data and simulation data are filtered using SAE-60 filter, for which the cut-off frequency is 100 Hz.

4.1. Full frontal impact

In full frontal impact simulations, the vehicle model impacted a stationary rigid wall at a prescribed impact velocity (Fig. 7(a)). For the validation of this model, the primary quantity of interest was the acceleration responses at the top and bottom of engine, and the left and right sides of the rear cross member. In one case the impact velocity of the model was 56.4 km/h (35 mph), corresponding to a NHTSA full frontal impact test of a two-door 1997 Honda Accord (number 2475 in NHTSA's vehicle crash test database). The acceleration responses from a simulation of the model and the physical test are illustrated in Fig. 8. The simulation results of the model basically match the timing, shape, and amplitude of the corresponding test signals.

In another case the impact velocity of the model was 48 km/h (30 mph), corresponding to a full frontal impact test of a four-door 1994 Honda Accord (number 2032 in NHTSA's database). The acceleration response comparisons for a computational simulation of the model and the physical test are illustrated in Fig. 9. The noticeable discrepancies between the simulation results and test data are suspected to be due to structural differences between 1997 and 1994 model.

The gross motions of the model and the test vehicle were also validated by comparing simulation animations with test videos. Good agreements were obtained. The gross motions of the model in the simulation of 35 mph impact at 32, 64, and 100 ms are shown in Figs. 7(b)–(d).

The agreement between the simulation results and test data for both impact velocities (30 and 35 mph) shows that the model has the capacity to predict acceleration responses as well as gross motions for the range of impact velocity.

4.2. Offset frontal impact

In the offset frontal impact, 40% of the vehicle width overlapped a honeycomb barrier and impacted it at 63.9 km/h (40 mph), as illustrated by Fig. 10(a). The barrier, supplemented with a ground plane, was stationary and deformable. The barrier was made of honeycomb material and wrapped with sheet metal.

The data of NHTSA test No. 2286 were used to validate simulation results. The physical test was conducted by the Insurance Institute for Highway Safety and the data were provided to NHTSA. Only the acceleration at the CG location of the vehicle was measured in the test. The simulation results and test data are displayed in Fig. 11(a)–(d) where the resultant and x-direction accelerations from the simulation and the test are in good agreement. The resultant acceleration needs to be computed because of the rigid body rotation of the vehicle during the impact. LS-DYNA outputs rigid body accelerations in the global coordinate system whereas the physical test recorded accelerations in the local coordinate system corresponding to the mounting of the accelerometer.

The gross motions of the model and the vehicle were also compared. The gross motions of the model are displayed in Figs. 10(b)–(d) for the 48, 100, 200 ms time-points.

4.3. Side impact

In the side impact simulations, the model was initially stationary and was impacted by a MDB that is traveling toward the vehicle at an initial velocity of 27.7 km/h (17.3 mph) in the x-direction and 54.3 (33.9 mph) in the y-direction (Fig. 12(a)). The corresponding physical test was a NHTSA side impact test of a four-door 1997 Honda Accord DX Sedan (Number 2479). The acceleration responses at the locations of vehicle's CG, front and rear right sill, and right rear cross member were used for validation. The simulation results and test signals for the right rear cross member and right front sill are illustrated in Figs. 13(a)–(d). It can be seen that in y-direction, the simulation results match well with the test results. The gross motions of the model are shown in Figs. 12(b)–(d) for the 32, 64, and 100 ms time-points.

It is concluded that the impact dynamic characteristics and kinematic behavior of the MDB have significant effects on the results of side impact simulations.

4.4. Oblique impact by a Ford Explorer

In this simulation, the Accord model was impacted frontally by the Explorer model at a 30° oblique angle from the center line, as shown in Fig 14(a). The Explorer model was developed by Oak Ridge National Laboratory. The initial velocities for the Accord model were $v_x =$ 56.5 km/h (35.3 mph), $v_y = 0$, and $v_z = 0$. The initial velocities for the Explorer model were $v_x = -48.5$ km/h (30.3 mph), $v_y = 28$ km/h (17.5 mph), and $v_z = 0$. The simulation was run for 100 ms. Figs. 14 (a)–(c) are overhead views of the Explorer obliquely impacting Accord at 0,40, and 100 ms.

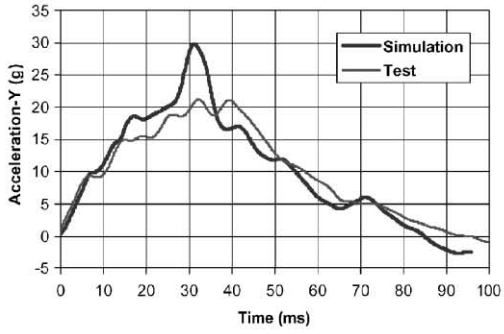

(a) Right rear cross member—Y

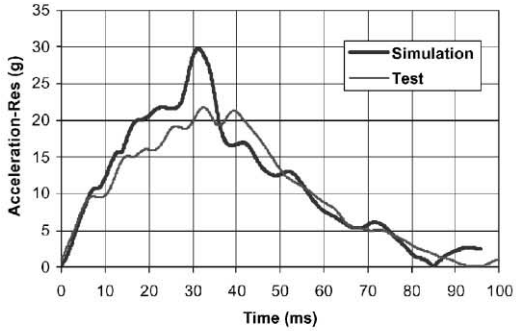

(b) Right rear cross member—Resultant

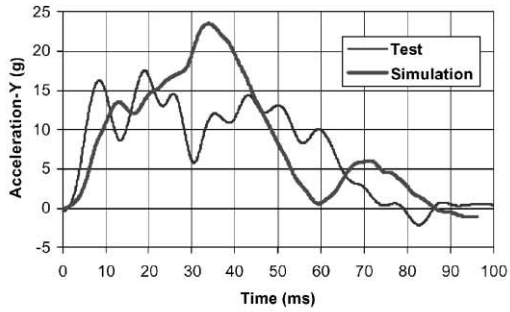

(c) Right front sill—Y

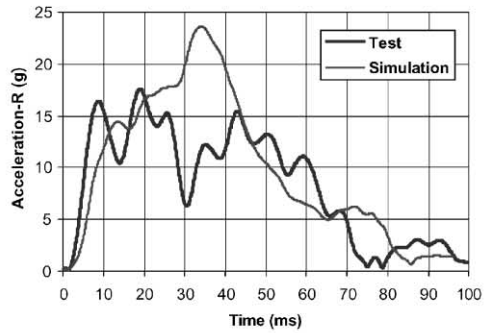

(d) Right front sill--Resultant

Fig. 13. Acceleration validation for the MDB 38 mph side impact.

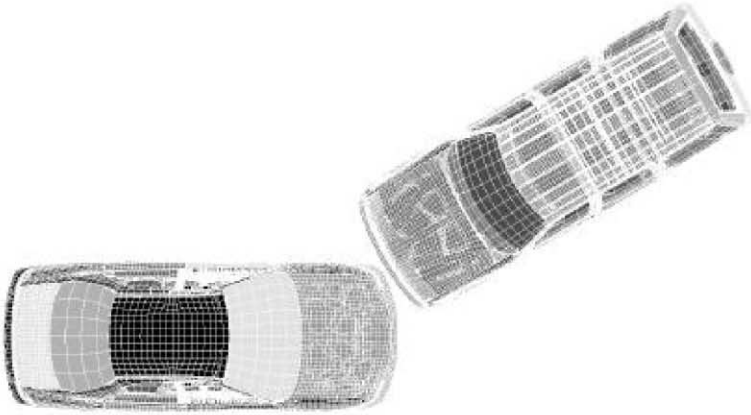

(a) t=0 ms

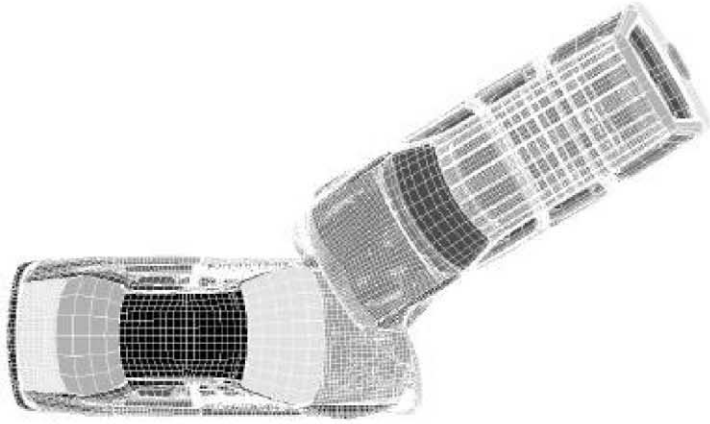

(b) t=40 ms

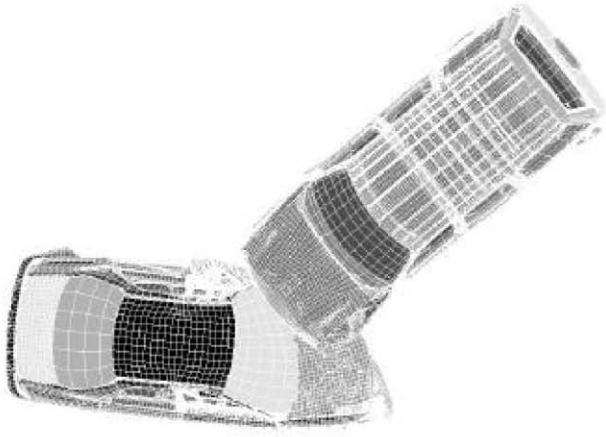

(c) t=100 ms

Fig. 14. Overhead view of Explorer obliquely impacting Accord.

5. Concluding remarks

A single finite element crash model has been developed for a four-door 1997 Honda Accord DX Sedan. This model has been successfully used in the simulations of the full frontal, offset frontal, side, and oblique car-to-car impacts. The results of computational simulations were validated with test data of actual vehicles. The validation indicates that the model is suitable for use as a crash partner for other vehicles. Computational tests of the model show that the model is computationally stable, reliable, and repeatable.

Acknowledgements

The work of developing a finite element model of the four-door 1997 Honda Accord DX Sedan was sponsored by the US National Highway Traffic Safety Administration (NHTSA). This was part of a joint industry–government program: Partnership for New Generation Vehicles.

References

[1] J. Fleck, New Car Assessment Program/Side Impact Testing/Passenger Cars/1997 Honda Accord/4-Door Sedan, NHTSA Report No. 214-MGA-97-01, MGA Research Corporation, WI, 1996.
[2] T.J.R. Hughes, The Finite Element Method, Linear Static and Dynamic Finite Element Analysis, Prentice-Hall, Inc., Englewood Cliffs, NJ, 1987.
[3] HyperMesh User's Manual, Version 2.1, Altair Computing, Inc., 1997.
[4] Livermore Software Technology Corporation, LS-DYNA Keyword User's Manual, Nonlinear Dynamic Analysis of Structures, Livermore, CA, 1999.
[5] J.G. Thacker, S.W. Reagan, J.A. Pellettiere, W.D. Pilkey, J.R. Crandall, E.M. Sieveka, Experiences during development of a dynamic crash response automobile model, Finite Element Anal. Des. 30 (1998) 279–295.